# Experimental investigation into the effects of diesel dilution on engine lubrication


## Abstract

The dilution of lubricant due to contamination with diesel fuel is an increasingly prevalent, potentially important and poorly understood issue. This study addresses two fundamental questions: 1) How does the change in lubricant rheology due to diesel dilution affect engine lubrication? 2) How is the chemical performance of lubricant components (base oil and performance additives) impacted by diesel dilution under different lubrication regimes (boundary/full film, hydrodynamic/elastohydrodynamic). This is achieved by testing three lubricant samples: 1) neat fully formulated 0W-30 engine oil, 2) fully formulated 0W-30 oil diluted with diesel at a concentration of 15%, denoted "0W-30D", and 3) neat, fully-formulated 0W-16, with the same base oil components and performance additives as the 0W-30, but blended to give a viscosity equal to that of the diluted an equivalent "0W-30D". Tribometer tests, including 1) low pressure, low shear viscosity, 2) Ultra-high Shear Viscosity (USV), 3) elastohydrodynamic film thickness, 4) Stribeck friction and 5) boundary friction and wear, are then conducted. To further emulate engine lubrication conditions, Stribeck curve measurements are performed on the three lubricants using a journal bearing test rig, fitted with a connecting-rod and commercial diesel engine shells. Results suggest that diesel dilution only slightly affects chemical additive performance (with friction modifiers being more inhibited than anti-wear additives) but does reduce both viscosity and film thickness. However, care must be taken in using viscometrics to predict dilution behaviour because 1) the pressure viscosity coefficient is also affected by diesel dilution which has implications for elastohydrodynamically lubrication contacts, 2) shear thinning means that viscosity modifier additives effects lose their functions at high shear rates; whereas diesel contamination affects viscosity behaviour throughout the whole shear rate range.



**Keywords:** diesel dilution, viscosity, journal bearings, friction, film thickness, hydrodynamic lubrication, shear thinning.

# Abbreviation

| | |
|---|---|
| EHD | Elastohydrodynamic |
| HFRR | High Frequency Reciprocating Rig |
| JBM | Journal Bearing Machine |
| MTM | Mini Traction Machine |
| RTD | Resistance Temperature Detector |
| SRR | Slide/Roll Ratio (in a ball-on-disc contact in the UTFI and MTM tests) |
| USV | Ultra Shear Viscometer |
| UTFI | Ultra-Thin Film Interferometry |
| VM | Viscosity-Modifier |
| ZDDP | Zinc dialkyldithiophosphate |

# Symbol

| | |
|---|---|
| $A'$ | EHD central film thickness at the entrainment speed of 1000 mm/s (nm) |
| $C$ | Walter constant in Walther mixing rule (cSt) |
| $E'$ | Reduced Young's modulus of the interacting solids in Dowson and Hamrock equation ($N/m^2$) |
| $F$ | Steady-state load applied on the connecting-rod in the JBM (N) |
| $f$ | Friction force between the bearing shells and the main shaft in the JBM (N) |
| $h_c$ | Central film thickness under the EHD lubrication (nm) |
| $k$ | Geometry-related constant of elliptical contact area in Dowson and Hamrock equation (-) |
| $T_{heater}$ | Temperature of the heater in the JBM (˚C) |
| $T_{journal}$ | Temperature of the journal bearing shells in the JBM (˚C) |
| $T_{lube}$ | Temperature of the inlet oil in the JBM (˚C) |
| $R'$ | Reduced radius of the interacting solids in Dowson and Hamrock equation (m) |
| $U$ | Entrainment speed in a ball-on-disc contact (m/s, in the UTFI and MTM tests) |
| $U_1$ | Speed of the ball in a ball-on-disc contact (m/s, in the UTFI and MTM tests) |
| $U_2$ | Speed of the disc in a ball-on-disc contact (m/s, in the UTFI and MTM tests) |
| $W$ | Applied load in a ball-on-disc contact (N) |
| $x$ | Volume fraction of lubricant in Walther mixing rule (%) |

| | |
|---|---|
| $\alpha$ | Pressure viscosity coefficient ($GPa^{-1}$) |
| $\dot{\gamma}$ | Shear rate of a lubricant ($s^{-1}$) |
| $\omega$ | Speed of the journal shaft in the JBM (rpm) |
| $\eta$ | Dynamic viscosity of lubricant specimens (cP) |
| $\eta_o$ | Dynamic viscosity of lubricant specimens at atmosphere pressure (cP) |
| $\eta_0$ | First Newtonian viscosity of lubricant specimens (cP) |
| $\eta_\infty$ | Second Newtonian viscosity of lubricant specimens (cP) |
| $\nu$ | Kinematic viscosity of lubricant specimens (cSt) |

# 1. Introduction

Fuel dilution (or crankcase dilution) refers to the phenomenon in which excessive and unburned engine fuel (diesel or gasoline) leaks into the crankcase and mixes with the engine lubricant [1]-[3]. Hydrocarbon-based engine fuel normally has lower viscosity than engine oil. This means that dilution may be beneficial in terms of engine efficiency due to lower viscous losses [4]-[5], but will also result in thinner oil films, increased surface contact between engine components (*e.g.* journal bearing shells/crankshaft, piston/liner), and this may lead to increased wear and even higher friction. Moreover, high temperatures and high pressures may facilitate chemical interaction between the fuel and the lubricant performance additives (*e.g.*, viscosity-modifier (VM) and anti-wear additives of zinc dialkyldithiophosphate (ZDDP) [6]), and could further affect lubrication characteristics.

Recent research in this area has focused on approaches to reduce fuel dilution and detect/monitor/quantify fuel dilution, and characterize the effect of different fuels [7]-[12]. For instance, high-frequency reciprocating tests, together with modelling have suggested that the presence of fuel in the cylinder liner contacts facilitates a transition from full-film, hydrodynamic lubrication to the undesirable boundary conditions due to reduced oil film thickness [9]. Tribometer testing of fuel diluted lubricants has also been combined with analytical ferrography to enable microscopic evaluation of wear debris [13]-[14]. More recently, biodiesel Fatty Acid Methyl Ester (FAME), has attracted attention as renewable and sustainable energy source, and its dilution of engine oil has been studied experimentally. Biodiesel is less volatile than other fuels and therefore its dilution effects are likely to more persistent under running engine conditions. This in contrast for instance to ethanol, which inhibits ZDDP film formation at low temperature but evaporates at 100 ℃ and has minimal tribological impact [15]. Four-ball and high frequency reciprocating testing has suggested that fresh biodiesel decreases friction forces in engine bearing shells, while aged-biodiesel degradation results in a chemical interaction with lubricant performance additives (mainly with the ZDDP) and leads to increased wear [15]. Furthermore, pin-on-disc tests quantifying wear under biodiesel-diluted lubrication conditions show that animal fat-based biodiesel can somewhat relieve the dilution effect, as compared to vegetable feedstock biodiesel [17]. Finally, the oxidation of biodiesel dilution in engine lubrication oil can increase deposits and accelerates corrosion, as indicated in [18].

A comprehensive understanding of the fuel dilution effect on lubrication performance is meaningful especially for car manufacturers, in terms of lubricant development and engine efficiency improvement. Two fundamental questions are proposed in the current study: 1) How do rheological changes due to fuel dilution effect engine lubrication? 2) How does diesel dilution effect the chemical performance of different lubricant components (base oil, and additives) under different lubrication regimes (boundary/hydrodynamic)? To address these, a

thorough experimental investigation is performed including a case study of diesel dilution in an engine journal bearing contact. Three lubricant samples are selected and tested: 1) neat, fully formulated 0W-30 engine oil, 2) fully formulated 0W-30 oil diluted with diesel at a concentration of 15%, denoted "0W-30D", and 3) neat, fully-formulated 0W-16, with the same base oil components and performance additives as the 0W-30, but blended to give a viscosity equal to that of the diluted equivalent "0W-30D". A series of tribometer tests, including Stabinger Viscometer, Ultra Shear Viscosity (USV), Ultra-Thin Film Interferometry (UTFI), Mini Traction Machine (MTM) and High Frequency Reciprocating Rig (HFRR), are performed to assess both rheological and tribological behaviour. Moreover, to emulate the journal bearing lubrication as operated in a real vehicle engine, a connecting-rod assembly from a diesel engine is modified to fit with a Journal Bearing Machine (JBM), and the Stribeck curve tests on the three lubricant samples are compared over a range of conditions.

This paper assesses the effects of diesel dilution on: 1) lubricant rheology in terms of viscosity and film thickness, considering both shear rate and pressure dependence – the latter being achieved by characterizing viscosity-pressure coefficients using a careful method compensating for physical uncertainties in contact geometries and material parameters, 2) chemical additive performance 3) automotive journal bearing friction under different regimes (boundary/mixed/hydrodynamic). This combined approach is necessary as overall engine efficiency depends on both the tribological and rheological [2] performance of a lubricant in various contacts operating under different regimes [3].

## 2. Lubricant Selection

To study the effect of fuel dilution on lubrication behaviour, three different lubricant samples are blended, as follows.

- Neat Shell Helix 0W-30 Ultra Professional AJ-L (denoted "0W-30" in the present work), which comprises base oil (Shell Risella X 420, a hydrocarbon fluid based on Shell Gas-to-Liquid technology) and performance additives (viscosity modifiers, anti-wear additives and so on), is a representative fully formulated lubricant and widely used in gasoline, diesel and gas engines.
- "0W-30" (as above), blended with diesel at a concentration of 15% by volume (denoted "0W-30D" in the present work).
- A research blend lubricant of "0W-16" (denoted "0W-16" in the present work), which has the same composition of base oil and performance additives as "0W-30", but contains a lower concentration of

viscosity modifier additive so as to give low pressure/low shear viscosity equal to that of the diesel diluted lubricant ("0W-30D").

Comparisons between test results from "0W-30D" and "0W-30" are intended to show the effects of fuel dilution on the lubrication performance, while test results from "0W-16" are intended to reveal whether the causes of discrepancies between "0W-30" and "0W-30D" are rheological or chemical in nature.

# 3. Tribometer Experiments

The three lubricants described above are characterized through a series of tests, as follows: 1) Low pressure/low shear viscosity, measured using Stabinger viscometer in order not only to quantify viscosity differences between the diluted and undiluted lubricants at low shear rate conditions, but also confirm that "0W-16" is correctly blended to have a viscosity equal to the diluted one; 2) High shear rate viscosity, measured using Ultra Shear Viscometer (USV), to characterize shear thinning behaviour; 3) Elastohydrodynamic (EHD) film thickness, measured using Ultra-Thin Film Interferometry (UTFI), to characterize pressure-viscosity coefficients; 4) EHD friction, measured using Mini Traction Machine (MTM), to characterize boundary, mixed friction and full film traction; and 5) boundary friction and wear volume, measured using High Frequency Reciprocating Rig (HFRR), to quantify tribological behaviour under harsh rubbing conditions.

Further details about these well-established measurement techniques can be found in [25], [26], [33] and [35].

## 3.1 Stabinger Viscometer

Stabinger viscometer measurement results of three lubricant, as well as the diesel, at low shear rate (10-100 $s^{-1}$) are listed in Table I in the Appendix and plotted in Figure 1, where each sample has been tested with the temperature swept from 20˚C to 100˚C. This shows that diesel dilution substantially reduces the viscosity of 0W-30, and also confirms that 0W-16 is correctly blended to a viscosity close to that of the diluted sample (0W-30D). The viscosity measurements have been linearly fitted with the Walther formula [36], written as:

$$\log_{10}(\log_{10}(\nu + 0.7)) = A - B \cdot \log_{10}(T) \quad (1)$$

where $\nu$ (cSt) is the kinematic viscosity, $T$ (K) is the temperature, and $A$ (= [8.23, 8.61, 9.14], for 0W-30, 0W-30D and 0W-16 respectively) and $B$ (= [3.21, 3.39, 3.60], for 0W-30, 0W-30D and 0W-16 respectively) are constants. It should be noted that the constant $B$ changes by only 5.45% when the 0W-30 is diluted (confirmed by the lines of the graph being approximately parallel), which shows that diesel dilution does not greatly affect the temperature dependence of the viscosity.

The expected kinematic viscosity of the diluted sample (0W-30D) can be also calculated by following Walther mixing rule as [36]-[37]:

$$\log_{10}(\log_{10}(\nu_{0W30D} + C)) = x_A \cdot \log_{10}(\log_{10}(\nu_{diesel} + C)) + x_B \cdot \log_{10}(\log_{10}(\nu_{0W30} + C)) \qquad (2)$$

where $x_A$ (= 0.15) and $x_B$ (= 0.85) are the volume fractions of the diesel and 0W-30 respectively, and $C$ (= 0.7) is Walther constant obtained via regression analysis. The predicted results, plotted as "0W-30D (Walther Mixing)" in Figure 1-(a), are in a good agreement with the Stabinger measured results. Moreover, Figure 1-(b) employs equation (2) again to essentially show how different concentrations of diesel affect the viscosity of the engine lubricant.

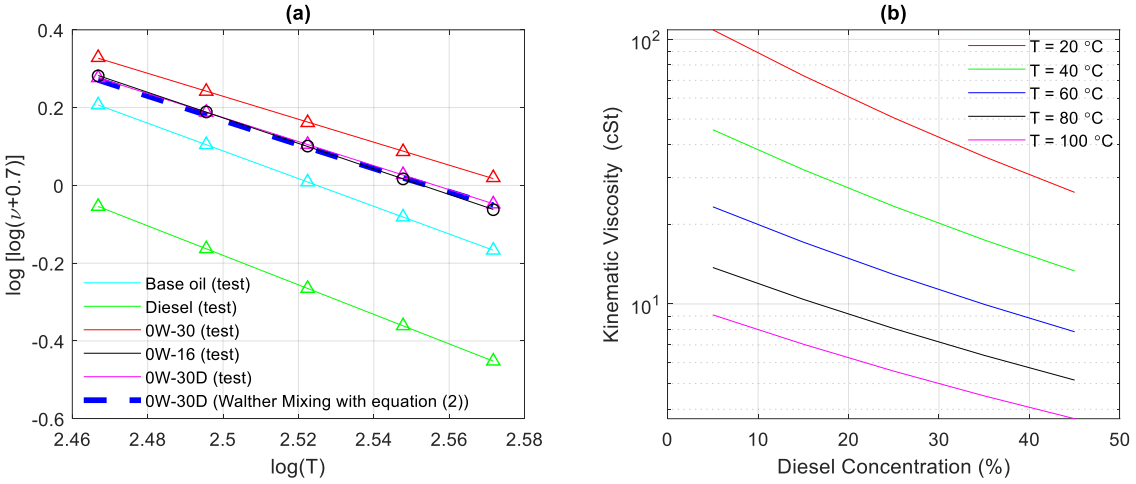



Figure 1: (a) Measurement results with the Stabinger Viscometer: kinematic viscosity ($\nu$, cSt) against the temperature ($T$, K) for the three selected lubricant samples as well as the base oil and the diesel. "0W-30D (Walther Mixing)" denotes the predicted kinematic viscosity of 0W-30D by following Walther Mixing rule in equation (2); (b) predicted kinematic viscosity of 0W-30 with different concentrations of diesel using Walther Mixing rule in equation (2).

## 3.2 Ultra-High Shear Viscosity Measurements

The Ultra Shear Viscometer (USV) from PCS Instruments [25], enables viscosity measurements at shear rates up to $10^7$ $s^{-1}$, without incurring significant shear heating and is commonly used to investigate shear thinning behaviour, *e.g.*, due to viscosity modifiers [20], [21].

The USV test results with the selected lubricant samples are shown in Figure 2, where the Carreau–Yasuda equation [19] is further employed to fit the viscosity versus shear rate at a given temperature:

$$\eta = \eta_\infty + (\eta_0 - \eta_\infty)(1 + (A\dot{\gamma})^a)^{\frac{n-1}{a}} \qquad (3)$$

where $\eta$ is the dynamic viscosity of the lubricant at the shear rate of $\dot{\gamma}$, $\eta_0$ is the first Newtonian viscosity, $\eta_\infty$ is the second Newtonian viscosity, while $A$, $a$ and $n \in [0.2, 0.9]$ are constants and are obtained through Matlab function *nlinfit*, as listed in Table II in the Appendix. The value of $\eta_\infty$ is normally close to the viscosity of the polymer-free formulation (the base oil). At 40˚C, the viscosity curves of 0W-30 and 0W-16 collapse into the horizontal line of the base oil at high shear rate (*i.e.* shear thinning has negated the effect of the viscosity modifier). By contrast, the viscosity of 0W-30D at high shear rate is the lowest, as it is determined jointly by both the base oil and the diesel, that is: $\eta_\infty$(0W-30) ≈ $\eta_\infty$(0W-16) > $\eta_\infty$(0W-30D), and $\eta_0$(0W-30) > $\eta_0$(0W-16) ≈ $\eta_0$(0W-30D).

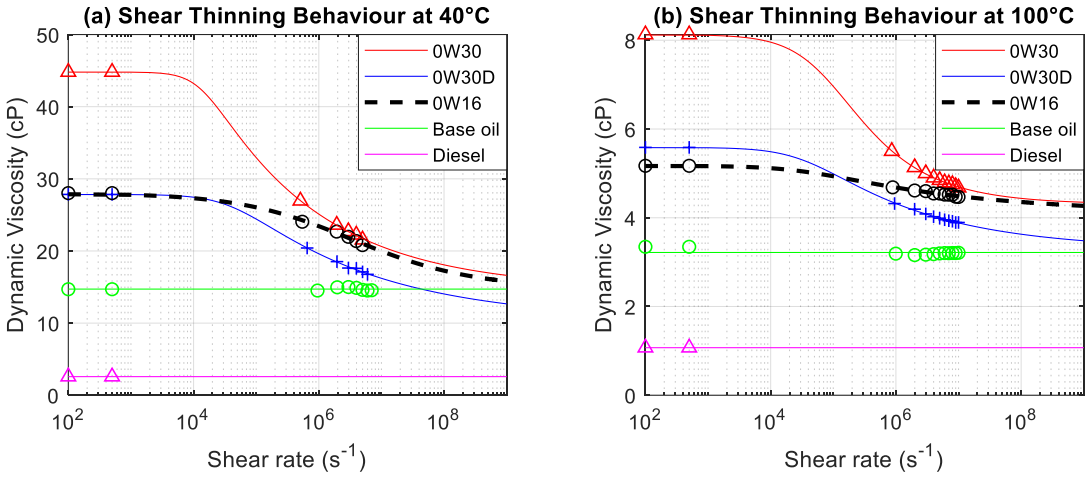



Figure 2: USV test results (markers) and equation fitting results (lines) for three lubricant samples as well as the base oil and the diesel: the variation of dynamic viscosity (cP) against shear rate ($s^{-1}$) at 40˚C (a) and 100˚C (b) respectively.

## 3.3 EHD Film Thickness Measurements

Ultra-Thin Film Interferometry (UTFI) is used to measure film thickness of lubricants under elastohydrodynamic (EHD) using optical interferometry. Here, a steel ball (the diameter of which is 19.05 mm) is loaded against a rotating glass disc, coated with a semi-reflective layer of chromium and silica [26]. The UTFI has an applicable measurement range of the oil film thickness within 1-1000 nm, with a load varying from 0 to 50 N, a contact pressure up to 0.7 GP.

UTFI tests with "0W-30", "0W-30D" and "0W-16" are performed at four different temperatures (40˚C, 60˚C, 80˚C and 100˚C), a constant applied load of 20 N, a varied entrainment speed of $U \in [4, 3000]$ mm/s (the entrainment speed is defined as $U = \frac{U_1+U_2}{2}$, where $U_1$ (mm/s) and $U_2$ (mm/s) are the speed of the ball and the disc respectively), and under pure rolling condition (i.e., $U_1 = U_2$, as the ball in the present test is not driven by the actuation shaft in the UTFI). The results of EHD central film thickness ($h_c$) against entrainment speed ($U$) are

shown in Figure 3, where it can be seen the film thickness of "0W-30" and "0W-16" have similar values, both of which are greater than that of the diluted lubricant.

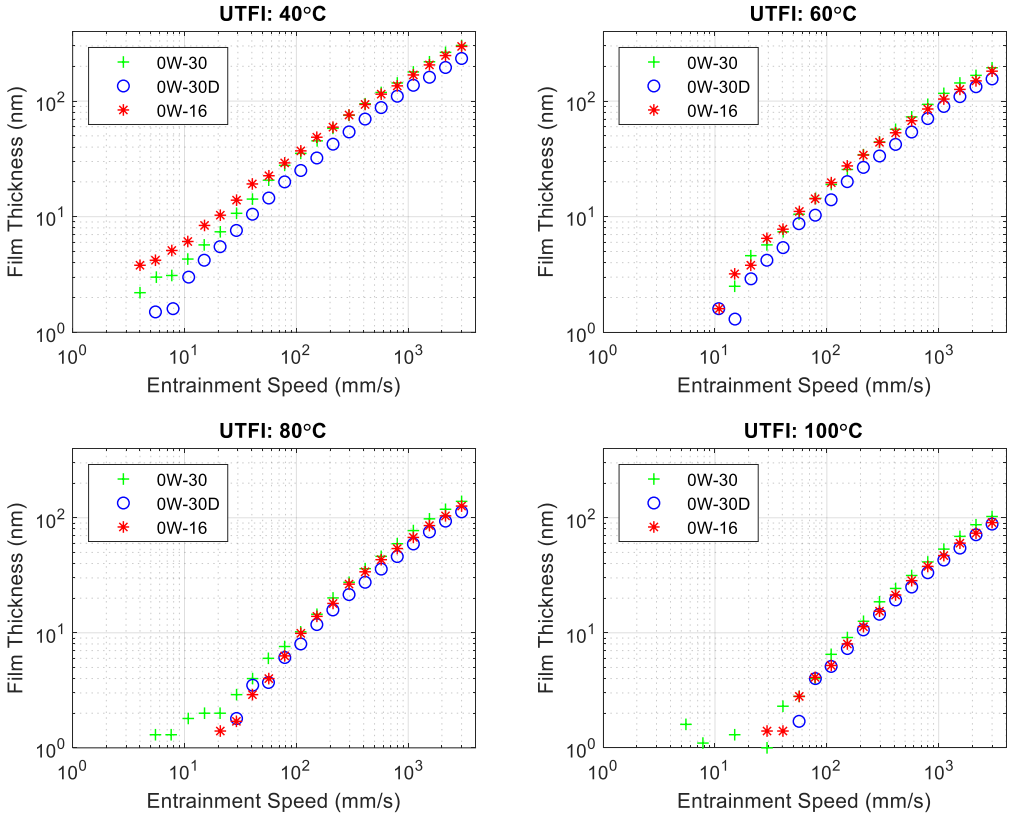



Figure 3: UTFI test results with three lubricant samples: the variation of the central film thickness ($h_c$) against the entrainment speed ($U$). (Note: the log scale underplays the differences between the samples at film thicknesses > 1nm).

To further understand the discrepancy in EHD film thickness ($h_c$) between the diluted and undiluted lubricants, Dowson and Hamrock equation, proposed in [27] and given as below, is employed:

$$h_c = kR'\left(\frac{U\eta_o}{E'R'}\right)^{0.68}(\alpha E')^{0.53}\left(\frac{W}{E'R'^2}\right)^{-0.067} = k'(U\eta_o)^{0.68}\alpha^{0.53} \quad (4)$$

where $k$ is determined by the geometry of elliptical contact area, $E'$ and $R'$ are the reduced Young's modulus and reduced radius of the interacting solids, $W$ is the applied load, $U$ is the entrainment speed of ball-on-disc contact, $\eta_o$ is the dynamic viscosity at atmosphere pressure, and $\alpha$ is the pressure viscosity coefficient. It is worth noting that Dowson and Hamrock equation is normally applied to Newtonian fluids with constant values of viscosity, while accurate EHD film thickness distribution of non-Newtonian fluids requires a much more complex numerical solution with exact profiles of shear stress - shear rate incorporated [28]-[30]. With respect to the present EHD tests of non-Newtonian fluids under pure-rolling condition, second Newtonian viscosity ($\eta_\infty$) is used instead in

Dowson and Hamrock equation to simplify the film thickness prediction meanwhile to minimize the calculation errors of the viscosity pressure coefficients ($\alpha$) [31].

Since three lubricant samples are tested under the same test conditions, the conventional Dowson and Hamrock equation can be further simplified as equation (4)-right side, with these lubricant-independent parameters collapsed into the constant, $k'$. This equation indicates the oil film variation is caused by both the lubricant viscosity $\eta_o$ and the pressure viscosity coefficient $\alpha$. $\eta_o$ has been replaced by the second Newtonian viscosity (i.e., $\eta_\infty$, the high shear rate viscosity as measured by the USV in Section 3.2) as discussed above, while the unknown parameters $\alpha$ can be accurately estimated as follows.

Firstly, a reference lubricant with known viscosity ($\eta_{oref}$) with known pressure viscosity coefficient ($\alpha_{ref}$) needs to be introduced and measured by the UTFI, again under exactly the same test conditions. The lubricant-independent constant, $k'$, which has significant uncertainties and may be inaccurately estimated, can be cancelled:

$$\frac{h_c}{h_{cref}} = \left(\frac{\eta_o}{\eta_{oref}}\right)^{0.68}\left(\frac{\alpha}{\alpha_{ref}}\right)^{0.53} \xrightarrow{yields} \alpha = \alpha_{ref}\left(\frac{\eta_o}{\eta_{oref}}\right)^{\frac{0.68}{0.53}}\left(\frac{h_{cref}}{h_c}\right)^{\frac{1}{0.53}} \tag{5}$$

where $h_{cref}$ is EHD central film thickness of the reference lubricant.

The measured data of both reference lubricant and the test samples, ($U$, $h_c$), can fit a linear equation with respect to $\log_{10} U$:

$$h_c = A' \cdot U^{0.68} \xrightarrow{yields} \log_{10} h_c = \log_{10} A' + 0.68 \cdot \log_{10} U \tag{6}$$

where the offset value of $A'$ can be approximated through Matlab function *polyfit*. It is worth noting that only the measured data ($U$, $h_c$) that satisfies $h_c$ > 10 nm are included here, despite the high measurement resolution of 1 nm given by the UTFI. This is due to the root-mean-square roughness ($R_q$) of the contact metal surface is around 10 nm, and the thin-film lubrication (< 10 nm) is in a regime of lubrication where the lubricant still flows but the value of film thickness can no longer be predicted by the conventional EHL model [32]. Since the value of $A'$ numerically equals $h_c$ at the entrainment speed of $U$ = 1000 mm/s (*i.e.*, $A' = h_c(U = 1)$ ), equation (5) can be further written as:

$$\alpha = \alpha_{ref}\left(\frac{\eta_o}{\eta_{oref}}\right)^{\frac{0.68}{0.53}}\left(\frac{h_{cref}(U_{ref} = 1000)}{h_c(U = 1000)}\right)^{\frac{1}{0.53}} = \alpha_{ref}\left(\frac{\eta_o}{\eta_{ref}}\right)^{\frac{0.68}{0.53}}\left(\frac{A'_{ref}}{A'}\right)^{\frac{1}{0.53}} \tag{7}$$

An example of linear fitting results with the UTFI measured data from the "0W-30" sample are displayed in Figure 4, and the calculation results of the pressure viscosity coefficients, $\alpha$, of three lubricant samples are listed in Table III in the Appendix and compared in Figure 5. The film thickness $h_c$(0W-30) ≈ $h_c$(0W-16) > $h_c$(0W-30D) and the pressure viscosity coefficients $\alpha$(0W-30) ≈ $\alpha$(0W-16) > $\alpha$(0W-30D). This finding, that it is only low-pressure viscosity but also the pressure viscosity coefficient that it is reduced as a result of diesel dilution, is likely to be because the molecular structure of the diesel is less branched than that of the base oil. The predicted pressure-viscosity coefficient and its dependence on diesel dilution are highly important as they are necessary to predict the viscometric characteristics of engine lubricants at different contact pressure, leading to the estimation of the film thickness distribution, for example, in gears, rolling element bearings and camshafts.

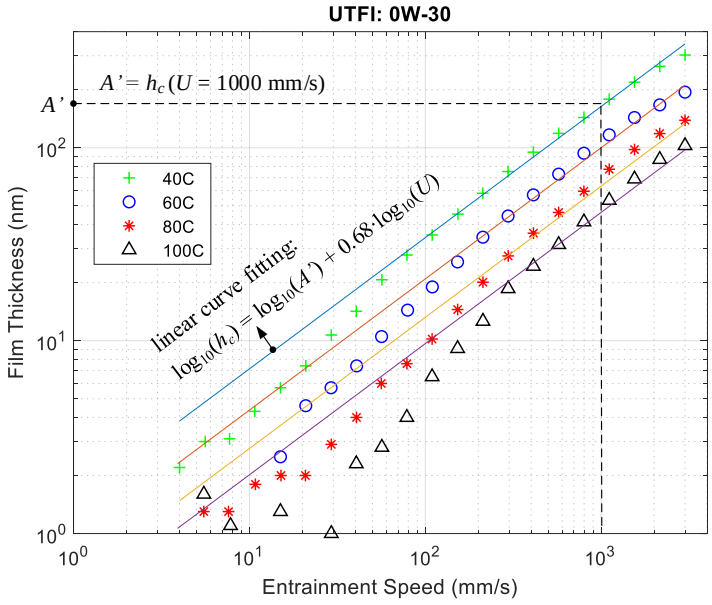



Figure 4 Linear fitting results of the UTFI measured data with the lubricant specimen "0W-30" (Note: the scatter in the data appears greater at low speed, however this is a result of the log scale which magnifies the nanometre variations).

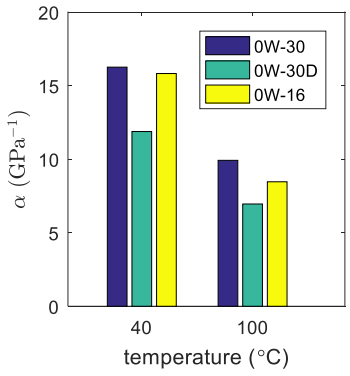



Figure 5 Comparison of the pressure viscosity coefficients, $\alpha$, between three lubricant samples.

## 3.4 Stribeck Friction under EHD conditions

A Mini Traction Machine (MTM), is used to measure EHL, mixed and boundary friction from a contact between a steel ball (19.05 mm diameter) and a steel disc (46 mm diameter), as detailed in [33].

Each lubricant sample is tested at four different temperatures (40 ˚C, 60 ˚C, 80 ˚C and 100 ˚C), the applied load is a constant value of 30 N, the ratio of the sliding speed to the entrainment speed, known as slide/roll ratio (SRR), is fixed at 50%, and the entrainment speed, $U$, is swept from 10 mm/s to 3500 mm/s. The MTM test results are presented in Figure 6, which all show a transition from mixed to EHD lubrication regime, showing that the "0W-30" and "0W-16" samples show similar friction values. This is because the shear rate ($>10^9$ $s^{-1}$, as estimated with the shear stress (the contact stress of around 0.5 GPa multiplied by the measured friction coefficients of 0.2-0.4) divided by the dynamic viscosity measured in the USV in Section 3.2) is sufficiently high throughout the MTM tests to cause shear thinning so the film thickness enhancing effect of the VM in the "0W-30" is negated. It is also the case that the both oils have the same chemical composition (in terms of base oil and surface active additives) and are therefore have similar boundary friction behaviour as expected [34]. The higher friction for the diesel diluted sample "0W-30D" can be attributed to two factors: firstly, the lower viscosity of this sample reduces the film thickness for a given entrainment speed and so increases the proportion of asperity contact in the mixed regime; on the other hand, the existence of diesel, which is a small size (around 1.8 nm) molecule with weak polarity, hinders the formulated polymer additives from bonding and acting on the contacting surfaces.

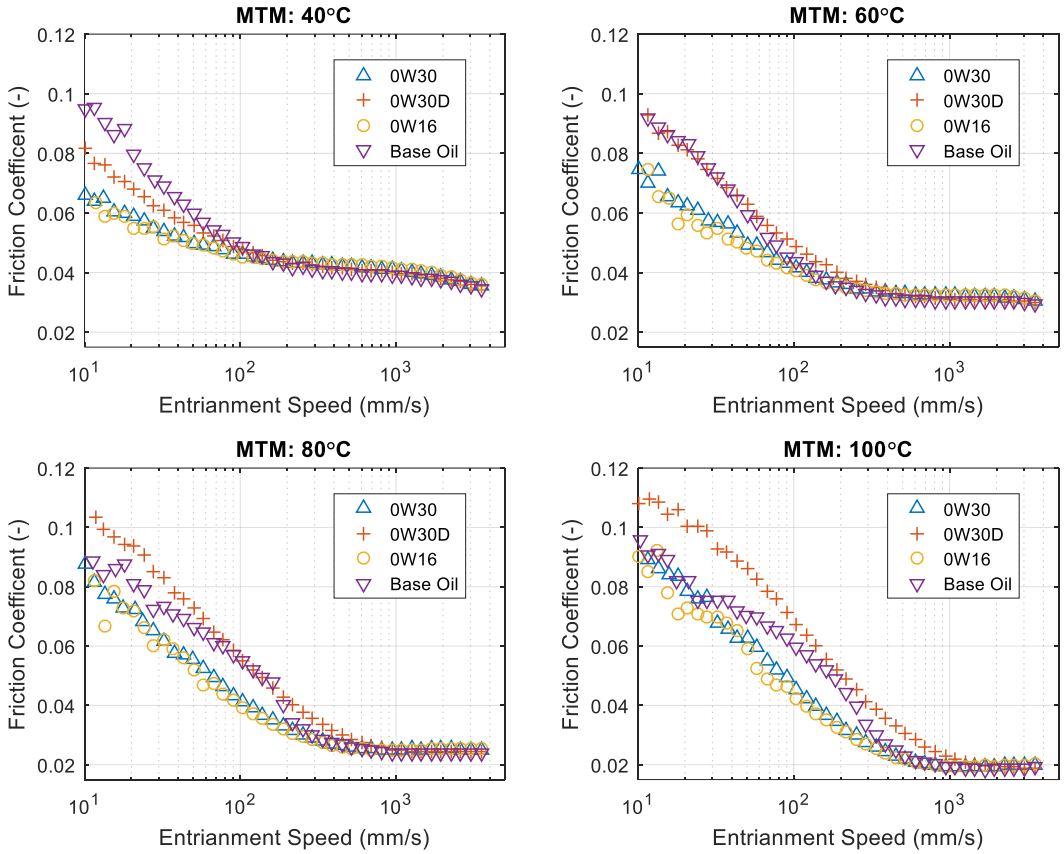



Figure 6: MTM test results with three lubricant specimens and their base oil: the variation of friction coefficients with respect to the entrainment speed ($U$).

## 3.5 High Frequency Reciprocating Rig (HFRR)

The High Frequency Reciprocating Rig (HFRR) producing a ball-on-flat contact is used to perform high-speed, reciprocating friction and wear tests under harsh rubbing conditions as described in [35]. A camera and microscope are then used to capture calibrated images of a wear scar. The HFRR has been widely used to assess the lubricity of diesel fuel [38] as well as the performance of surface additives (e.g., the anti-wear additive ZDDP).

HFRR testing of "0W-30", "0W-30D" and "0W-16" is performed under the conditions of 2 hour rubbing time, 100 ˚C temperature, 50 Hz reciprocating motion, and 400 g load. The test results are shown in Figure 7 and Figure 8, where it can be seen both the friction coefficients and wear volumes (quantified by wear scar dimensions) of three lubricant specimens are almost identical, while their base oil exhibits the highest values. This suggests diesel dilution only slightly affects the anti-wear performance of surface additives.

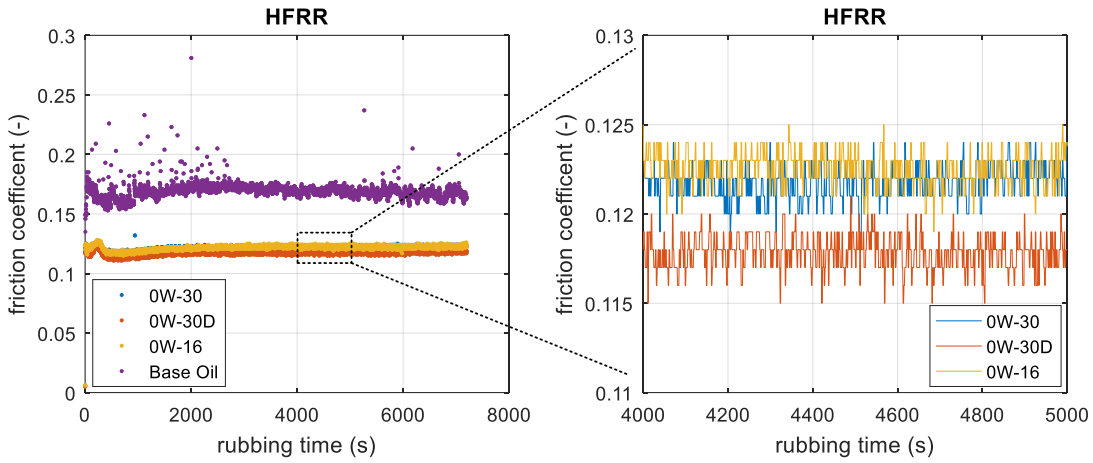



Figure 7: HFRR test results with three lubricant samples and their base oil: the variation of friction coefficient with respect to rubbing time.

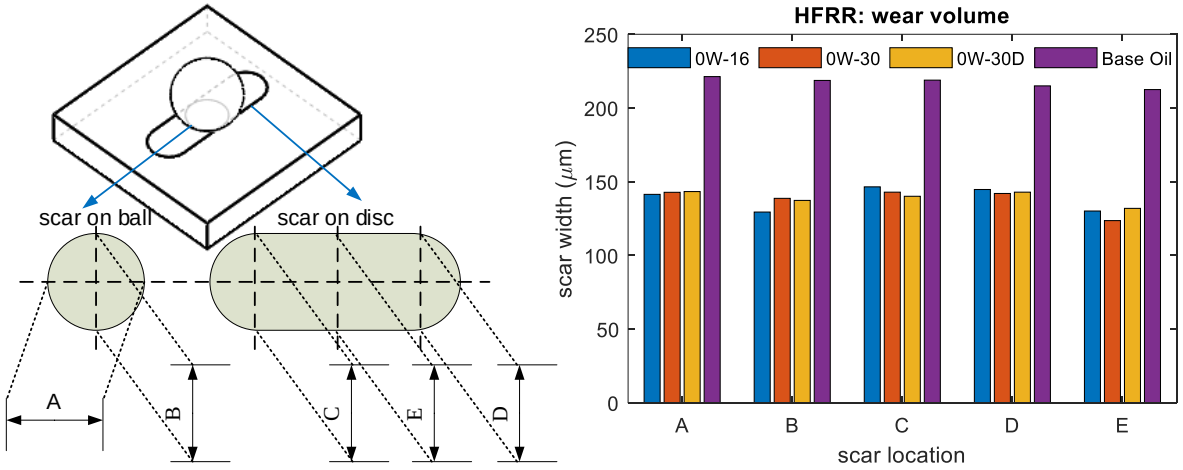


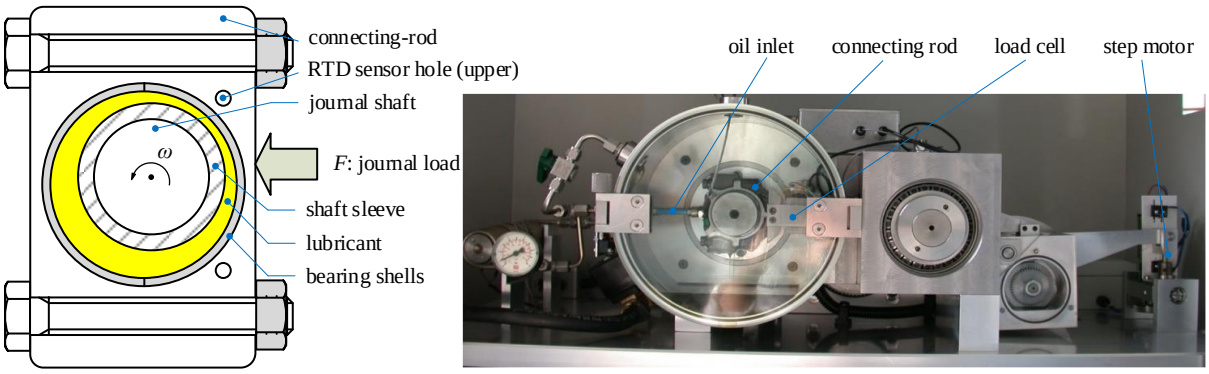

Figure 8: HFRR test results with three lubricant samples and their base oil: (left) illustration of scar shapes in the ball and the disc respectively; (right) scar dimensions at different locations.

## 4. Journal Bearing Machine Experiments

To emulate lubrication conditions under a real crankshaft-journal bearing operating environment, in this section, a connecting-rod assembly is modified to fit a journal bearing machine (JBM, which has been employed previously to experimentally study the effects of viscosity-modifiers (VMs) and laser surface texture on journal bearing lubrication [22], [23]), such that friction force measurements and comparison between different lubricant samples can be realistic.

## 4.1 Setup of Journal Bearing Machine (JBM)

To fit the connecting-rod from a diesel engine into the JBM test rig, a hollow shaft sleeve is utilized and fixed onto the journal shaft through an interference fit, the out diameter of the shaft sleeve (the nominal dimension is 55 mm) is designed to have a desirable dimension clearance (50 μm) that matches the target bearing shells, as shown in Figure 9-a). The connecting-rod is further modified by cutting its beam, such that the produced flat section facilitates the connection of the load cell of the JMB, as shown in Figure 9-b).




a) b)

Figure 9: a) schematic of modified connecting-rod assembly and b) the journal bearing machine (JBM).

The JBM is equipped with the following actuators: i) A stepping motor, which provides a steady-state load ($F$) to the connecting rod; ii) A cam-driven motor, which provides a periodical load to the connecting rod as the classical four-stroke engine does; iii) A primary journal motor, which derives the journal shaft to emulate the crankshaft rotation in an engine; iv) An oil pump motor, which pumps oil to the journal bearing chamber.

The JBM is equipped with the following sensors: i) A load cell, which measures the lateral load ($F$) and the friction force ($f$) of the journal bearing; ii) An internal encoder, which measures the journal shaft velocity ($\omega$); iii) Three RTDs (resistance temperature detectors), which are installed respectively for the temperature measurement of at the oil system heater ($T_{heater}$), the chamber inlet oil ($T_{lube}$), and the bearing shells ($T_{journal}$). In addition, a couple of control schemes are in place: i) Closed-loop controllers that enable reference value tracking of the lateral load, $F$, with the step motor position being the manipulated control variable; ii) Reference value tracking of the chamber inlet oil temperature, $T_{lube}$, with the heater being the manipulated device; iii) Reference value tracking of the journal shaft speed, $\omega$, which is implemented by an inner-loop PI controller for the journal motor.

The nominal operation ranges are as follows: the steady-state load of the connecting-rod $F \in [1, 10]$ kN, the temperature of the chamber inlet oil $T_{lube} \in [60, 120]$ ˚C, and the journal shaft speed $\omega \in [750, 3500]$ rpm.

## 4.2 Test Procedures and Results with Journal Bearing Machine (JBM)

To remove bearing asperities and ensure repeatability of experimental results between different lubricant samples, a running-in step should be performed, after each the substitution of a new pair of bearing shells [23]. The running-in test conditions are given by the harshest conditions during the subsequent tests, and empirically located between the EHD and mixture lubrication regimes to avoid excessive friction and wear. In the present experiment, they are identified as:

- Step 1: chamber inlet oil temperature $T_{lube}$ = 80 ˚C, the journal load $F$ = 3 kN, the journal speed $\omega$ = +750 rpm, duration = 18 mins;
- Step 2: same as Step 1 above, while performs a reverse journal speed $\omega$ = -750 rpm.

The formal test conditions for each lubricant specimen are detailed as follows:

- Step 1: an 18 min time step with constant parameters of: the inlet oil temperature $T_{lube}$ = 60 ˚C, the journal load $F$ = 3 kN, and the journal speed $\omega$ = 3000 rpm, the results of which are shown in Figure A.I-left in the Appendix. This step aims to stabilize the temperature of the journal bearing shells, $T_{journal}$, which has the closest value to that of the lubricant film between the journal shaft sleeve and bearing shells (no closed-loop control for the tracking of $T_{journal}$ is placed in the JBM);
- Step 2: the inlet oil temperature $T_{lube}$ = 60 ˚C, the journal load $F$ = 1 kN, and the journal speed is swept within $\omega$ = [750, 1000, 1250, 1500, 2000, 2500, 3000, 3500] rpm (both forward and reverse directions are performed for each speed value to compensate floating signal offsets in the friction torque/force measurements);
- Step 3: the inlet oil temperature $T_{lube}$ = 60 ˚C, the journal load $F$ = 3 kN, and the journal speed $\omega$ is swept in the same range as Step 2;
- Step 4: repeat Step 1 to Step 3 with all $T_{lube}$ changed form 60 ˚C to 80 ˚C;
- Step 5: repeat Step 1 to Step 2 with all $T_{lube}$ changed form 60 ˚C to 100 ˚C (the journal load $F$ = 3 kN is not applied under high temperature conditions to avoid excessive wear in the boundary lubrication regime).

The repeatability of the JBM test results are demonstrated by two representative groups of friction force measurements, as shown in Figure 10, where the first round of friction force measurements essentially agree with these in the second round throughout the journal speed range. Figure 10 also shows that the effect of dilution as expected is to i) reduce friction in the full film hydrodynamic regime due to reduced viscous shear and ii) increase friction in the mixed regime due to reduced hydrodynamic lift. It should be noted that, in terms of machine efficiency, the latter effect is especially important since the reduction in friction occurs at high speed where more energy is dissipated. This suggests that in some cases, diesel dilution may actually be beneficial in increasing efficiency and reducing fuel consumption, providing the effects of wear in the mixed and boundary regimes are limited.

The final comparison results between three lubricant samples are presented in Stribeck curves, where *y*-axis is the friction coefficient (the ratio of the friction force $f$ to the steady-state load $F$) and *x*-axis is the "lubricant viscosity (cP) × the journal speed (rpm) / the journal load (N)" (i.e., $\frac{\eta \cdot \omega}{F}$), as shown in Figure 11. In the hydrodynamic lubrication regime, the diluted specimen "0W-30D" presents a shift to the left as compared to "0W-30", while "0W-30D" is closely aligned with "0W-16", thus the diesel dilution effect in this regime is purely a reduction in lubricant viscosity. In the mixed lubrication regime, the friction coefficient variation of the three specimens are not well collapsed into the same curve. This is due to the fully formulated (with polymer additives) engine lubricants are non-Newtonian fluids. On the other hand, the diluted lubricant "0W-30D" has higher friction coefficient than that of "0W-30" and "0W-16", which essentially corresponds to the MTM test results (in Subsection 3.4), and is due to the existence of diesel hindering the formulated surface additives from bonding and acting on the contacted surfaces.

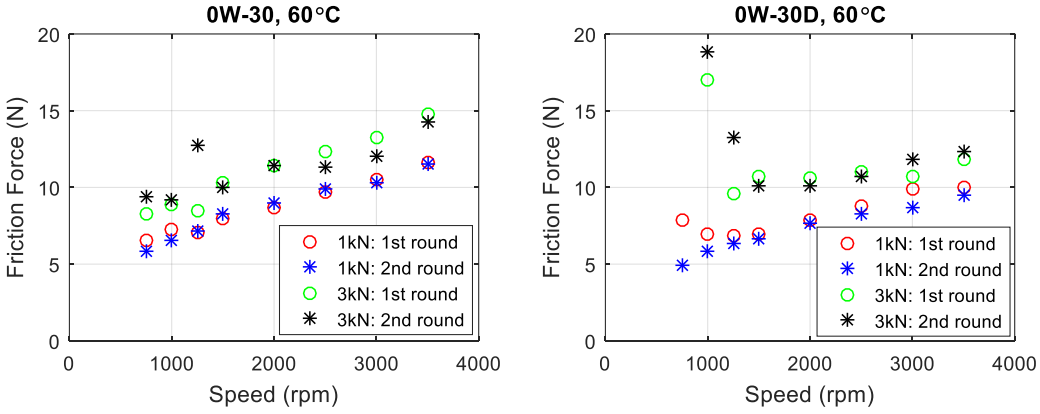



Figure 10: Repeatability assessment with two representative groups of JBM test results. The left plot is with the "0W-30" test fluid at the inlet oil temperature $T_{lube}$ = 60˚C, while the right one is with the specimen "0W-30D" at $T_{lube}$ = 60˚C.

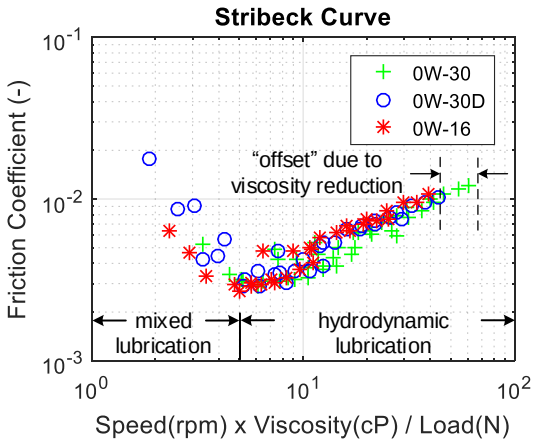



Figure 11: JBM test results, as presented in Stribeck Curves, with lubricant specimens of "0W-30", "0W-30D" and "0W-16".

# 5. Discussion and Conclusions

This paper experimentally investigates how the diesel dilution affects engine lubrication performance, with three lubricant tested: 1) fully formulated engine oil "0W-30", 2) diluted "0W-30" with 15% diesel fuel blended (denoted as "0W-30D"), and 3) "0W-16", which has the same composition "0W-30" but is blended in different proportions to have an equivalent viscosity to "0W-30D".

A group of tribometer tests are performed to show the discrepancy between three samples, in terms of tribological and rheological characteristics: 1) The test results with the Stabinger Viscometer, on one hand, show the 15% diesel dilution results in a significant reduction of viscosity to "0W-30", from 44.81 cSt to 27.84 cSt at 40˚C and also validate the "0W-16" as being correctly blended to viscosity similar to that of the diluted sample "0W-30D". 2) The test results with Ultra Shear Viscometer (USV) show how the shear thinning behaviour of engine lubricant is influenced by the diesel dilution – specifically the viscosities of "0W-30" and "0W-16" collapse to a single value at high shear rates ($> 5 \times 10^{-6}$ $s^{-1}$), where the polymer additives only slightly contribute to the viscosity; whereas diesel contamination affects viscosity behaviour throughout the whole shear rate range, since in the high shear rate regime the sample "0W-30D" has the lowest viscosity value, which is determined by both the base oil and the diesel. 3) The test results with the Ultra-Thin Film Interferometry (UTFI) show the variation of oil film thickness in the elastohydrodynamic (EHD) regime, where "0W-30D" presents the thinnest oil film and in agreement with the above shear thinning analysis. Furthermore, analysis of the film thickness data show that diesel dilution also effects the pressure-viscosity coefficient of the lubricant 4) The test results with the Mini Traction Machine (MTM) show "0W-30D" has highest friction coefficients in the mixed lubrication regime, while "0W-30" and "0W-16" have similar responses. This is suggested to result from a combination of viscosity

reduction causing an increase in asperity contact and also a slight inhibition of friction reducing boundary film formation due to the small, weakly polar diesel molecule 5) High Frequency Reciprocating Rig (HFRR) performs harsh rubbing conditions and the results show only slight difference between three lubricant samples, in terms of the wear scar and the friction coefficient, which indicate the diesel dilution does not affect the anti-wear additives.

To emulate lubrication environment as in a real engine journal bearing and to obtain, a connecting-rod from a diesel engine is modified to fit a journal bearing machine (JBM) and tested with the three lubricant samples. The results of which are presented and compared in the form of Stribeck curves. Overall, the key conclusions that can be drawn are listed as follows.

- In the hydrodynamic lubrication regime, the Stribeck curve of the diluted "0W-30D" is closely aligned with that of "0W-16", while individual values shifted to the left as compared to "0W-30". Therefore, under these conditions, diesel dilution effect is solely a reduction in the lubricant viscosity and this may be compensated for by using viscosity modifier additives.
- At high shear rates, shear thinning means that viscosity modifier additives effects lose their functions. Under these conditions, viscosity is determined by the base oil and any diesel dilution. Therefore, "0W-30" and "0W-16" show similar high shear rate behaviour with thicker lubricants films than the diesel diluted sample, as shown by the UTFI test results.
- In the mixed lubrication regime, MTM results indicate that "0W-30" and "0W-16" have similar response in terms of the variation of friction coefficient, while "0W-30D" shows highest friction. This suggests that the existence of diesel hinders polymer additives bonding and acting on the contacted surfaces.
- In the boundary lubrication regime, the diesel dilution does not affect the surface additives, as three lubricants present almost identical fiction coefficients and wear volumes under harsh rubbing conditions, while much less than the base oil does.

# Appendix

Table I Measurement results of kinematic viscosity (cSt) with Stabinger Viscometer

| | 40 ˚C | 60 ˚C | 80 ˚C | 100 ˚C |
|---|---|---|---|---|
| 0W-30 | 54.82 | 27.45 | 15.92 | 10.42 |
| 0W-30D | 34.04 | 18.10 | 10.93 | 7.16 |
| 0W-16 | 34.34 | 17.57 | 10.24 | 6.64 |
| Base oil* | 18.01 | 9.78 | 6.04 | 4.10 |
| Diesel | 3.08 | 2.16 | 1.62 | 1.28 |

* The same base oil of 0W-30 and 0W-16: Shell Risella X 420.

Table II Carreau–Yasuda constants as fitted with ultra shear viscometer (USV) measurement results

| | 40 ˚C | | | 100 ˚C | | |
|---|---|---|---|---|---|---|
| | $A$ | $a$ | $n$ | $A$ | $a$ | $n$ |
| 0W-30 | 77.03 | 2.07 | 0.76 | 12.60 | 1.07 | 0.53 |
| 0W-30D | 24.10 | 1.30 | 0.80 | 27.56 | 1.14 | 0.76 |
| 0W-16 | 0.47 | 0.50 | 0.60 | 27.47 | 0.92 | 0.82 |

Table III Comparison of EHD central film thickness at the entrainment speed of 1000 mm/s ($A'$) and pressure viscosity coefficients ($\alpha$)

| | 40 ˚C | | 100 ˚C | |
|---|---|---|---|---|
| | A’ (nm) | $\alpha$ (GPa$^{-1}$) | A’ (nm) | $\alpha$ (GPa$^{-1}$) |
| Reference oil | 93 | 12.54 | 33 | 9.37 |
| 0W-30 | 164 | 16.26 | 46 | 9.92 |
| 0W-30D | 121 | 11.88 | 35 | 6.95 |
| 0W-16 | 161 | 15.82 | 43 | 9.42 |

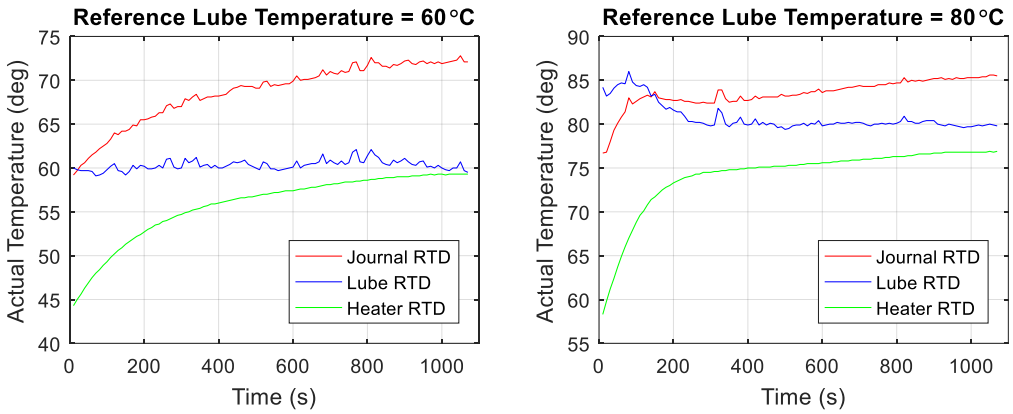



Figure A.I: An 18 mins time step for the stabilization of the journal bearing temperature $T_{journal}$, with the reference value of the inlet oil temperature $T_{lube}$ being 60 ℃ (left) and 80 ℃ (right) respectively. The variables depicted include the actual values of the journal bearing temperature $T_{journal}$, the inlet oil temperature $T_{lube}$, and the JBM heater temperature $T_{heater}$.

# Reference


[1] Wilson, R. E., & Wilkin, R. E. (1926). *A Suggested Remedy for Crankcase-Oil Dilution* (No. 260006). SAE Technical Paper.
https://doi.org/10.4271/260006

[2] Taylor, R. I. (1997). Engine friction: the influence of lubricant rheology. *Proceedings of the Institution of Mechanical Engineers, Part J: Journal of Engineering Tribology*, *211*(3), 235-246.
https://doi.org/10.1177/135065019721100306

[3] Holmberg, K., Andersson, P., & Erdemir, A. (2012). Global energy consumption due to friction in passenger cars. *Tribology international*, *47*, 221-234.
https://doi.org/10.1016/j.triboint.2011.11.022

[4] Korcek, S., Sorab, J., & Jensen, R. K. (2000). Automotive lubricants for the next millennium. *Industrial Lubrication and tribology*.
https://doi.org/10.1108/00368790010373175

[5] Maci án, V., Tormos, B., Berm údez, V., & Ram írez, L. (2014). Assessment of the effect of low viscosity oils usage on a light duty diesel engine fuel consumption in stationary and transient conditions. *Tribology International*, *79*, 132-139.
https://doi.org/10.1016/j.triboint.2014.06.003

[6] Passut, C. A. (2013). Engine Lubricants. *Encyclopedia of Tribology*, 977-981.
https://doi.org/10.1007/978-0-387-92897-5

[7] Niedermayer, A. O., Voglhuber-Brunnmaier, T., Heinisch, M., Feichtinger, F., & Jakoby, B. (2016). Monitoring of the dilution of motor oil with diesel using an advanced resonant sensor system. *Procedia Engineering*, *168*, 15-18.
https://doi.org/10.1016/j.proeng.2016.11.116

[8] Song, B. H., & Choi, Y. H. (2008). Investigation of variations of lubricating oil diluted by post-injected fuel for the regeneration of CDPF and its effects on engine wear. *Journal of Mechanical Science and Technology*, *22*(12), 2526-2533.
https://doi.org/10.1007/s12206-008-0903-x

[9] Smith, O., Priest, M., Taylor, R. I., Price, R., Cantlay, A., & Coy, R. C. (2006). Simulated fuel dilution and friction-modifier effects on piston ring friction. *Proceedings of the Institution of Mechanical Engineers, Part J: Journal of Engineering Tribology*, *220*(3), 181-189.
https://doi.org/10.1243%2F13506501JET162

[10] Hu, T., Teng, H., Luo, X., Lu, C., & Luo, J. (2015). *Influence of fuel dilution of crankcase oil on ignitability of oil particles in a highly boosted gasoline direct injection engine* (No. 2015-01-2811). SAE Technical Paper.
https://doi.org/10.4271/2015-01-2811

[11] Nanjundaswamy, H., Tatur, M., Tomazic, D., Koerfer, T., Lamping, M., & Kolbeck, A. (2009). *Fuel property effects on emissions and performance of a light-duty diesel engine* (No. 2009-01-0488). SAE Technical Paper.
https://doi.org/10.4271/2009-01-0488

[12] Barnard, D., & Fleming, R. (1967). The Effect of Evaporative Cooling in Saddle Fuel Tanks on Diesel Engine Operation. In *Diesel Fuel Oil*. ASTM International, 25-41.
https://doi.org/10.1520/STP46056S

[13] Singh, P., Goel, V., & Chauhan, S. R. (2017). Impact of dual biofuel approach on engine oil dilution in CI engines. *Fuel*, *207*, 680-689.
https://doi.org/10.1016/j.fuel.2017.06.110

[14] Agarwal, A. K., Bijwe, J., & Das, L. M. (2003). Effect of biodiesel utilization of wear of vital parts in compression ignition engine. *J. Eng. Gas Turbines Power*, *125*(2), 604-611. https://doi.org/10.1115/1.1454114

[15] Costa, H. L., & Spikes, H. A. (2016). Impact of ethanol on the formation of antiwear tribofilms from engine lubricants. *Tribology International*, *93*, 364-376. https://doi.org/10.1016/j.triboint.2015.09.021

[16] Fang, H. L., Whitacre, S. D., Yamaguchi, E. S., & Boons, M. (2007). *Biodiesel impact on wear protection of engine oils* (No. 2007-01-4141). SAE Technical Paper. https://doi.org/10.4271/2007-01-4141

[17] Shanta, S. M., Molina, G. J., & Soloiu, V. (2011). Tribological effects of mineral-oil lubricant contamination with biofuels: a pin-on-disk tribometry and wear study. *Advances in Tribology*, *2011*. https://doi.org/10.1155/2011/820795

[18] Gili, F., Igartua, A., Luther, R., & Woydt, M. (2011). The impact of biofuels on engine oil performance. *Lubrication Science*, *23*(7), 313-330. https://doi.org/10.1002/ls.158

[19] Yasuda, K. Y., Armstrong, R. C., & Cohen, R. E. (1981). Shear flow properties of concentrated solutions of linear and star branched polystyrenes. *Rheologica Acta*, *20*(2), 163-178. https://doi.org/10.1007/BF01513059

[20] Marx, N., Fernández, L., Barceló, F., & Spikes, H. (2018). Shear thinning and hydrodynamic friction of viscosity modifier-containing oils. Part I: shear thinning behaviour. *Tribology Letters*, *66*(3), 92. https://doi.org/10.1007/s11249-018-1039-5

[21] Marx, N., Fernández, L., Barceló, F., & Spikes, H. (2018). Shear thinning and hydrodynamic friction of viscosity modifier-containing oils. Part II: impact of shear thinning on journal bearing friction. *Tribology Letters*, *66*(3), 91. https://doi.org/10.1007/s11249-018-1040-z

[22] Vladescu, S. C., Marx, N., Fernández, L., Barceló, F., & Spikes, H. (2018). Hydrodynamic friction of viscosity-modified oils in a journal bearing machine. *Tribology Letters*, *66*(4), 127. https://doi.org/10.1007/s11249-018-1080-4

[23] Vlădescu, S. C., Fowell, M., Mattsson, L., & Reddyhoff, T. (2019). The effects of laser surface texture applied to internal combustion engine journal bearing shells–an experimental study. *Tribology International*, *134*, 317-327. https://doi.org/10.1016/j.triboint.2019.02.009

[24] Jacobson, B. (2003). The Stribeck memorial lecture. *Tribology International*, 36(11), 781-789. https://doi.org/10.1016/S0301-679X(03)00094-X

[25] USV: high shear rate of viscosity measurements. https://pcs-instruments.com/product/usv/

[26] UTFI: oil film thickness measurements. https://pcs-instruments.com/product/ehd-elasto-hydrodynamic-lubriction-2/

[27] Hamrock, B. J., & Dowson, D. (1976). Isothermal elastohydrodynamic lubrication of point contacts: Part 1—Theoretical formulation. https://doi.org/10.1115/1.3452801

[28] Bair, S., & Khonsari, M. (1996). An EHD inlet zone analysis incorporating the second Newtonian. *J. Tribology*, 118. 341-343.

[29] Bair, S., & Winer, W. O. (1997). A simple formula for EHD film thickness of non-Newtonian liquids. In *Tribology Series* (Vol. 32, pp. 235-241). Elsevier.

[30] Bair, S. (1998). Elastohydrodynamic film forming with shear thinning liquids.

[31] Greenwood, J. A., & Kauzlarich, J. J. (1998). Elastohydrodynamic film thickness for shear-thinning lubricants. *Proceedings of the Institution of Mechanical Engineers, Part J: Journal of Engineering Tribology*, 212(3), 179-191. https://doi.org/10.1243%2F1350650981541994

[32] Y.-Z. Hu, T.-B. Ma. (2011) Tribology of Nanostructured Surfaces, Comprehensive Nanoscience and Technology, Academic Press, 383-418, https://doi.org/10.1016/B978-0-12-374396-1.00116-1

[33] MTM: Friction and tracking force measurement. https://pcs-instruments.com/product/mtm/

[34] Neveu, C. D., Sondjaja, R., Stöhr, T., Schimossek, K., & Iroff, N. J. (2016). Lubricant and fuel additives based on polyalkylmethacrylates, *Reference Module in Materials Science and Materials Engineering, Elsevier*. https://doi.org/10.1016/B978-0-12-803581-8.01544-7

[35] HFRR: high-frequency reciprocating tests. https://pcs-instruments.com/product/hfrr-high-frequency-reciprocating-rig

[36] Walther, C. (1931). The evaluation of viscosity data. *Erdol Teer*, *7*, 382-384.

[37] Centeno, G., Sánchez-Reyna, G., Ancheyta, J., Muñoz, J. A., & Cardona, N. (2011). Testing various mixing rules for calculation of viscosity of petroleum blends. *Fuel*, *90*(12), 3561-3570. https://doi.org/10.1016/j.fuel.2011.02.028

[38] Zhang, J., Yamaguchi, E., & Spikes, H. (2013). Comparison of three laboratory tests to quantify mild wear rate. *Tribology transactions*, 56(6), 919-928. https://doi.org/10.1080/10402004.2013.807530

[39] Marinescu, I. D., Rowe, W. B., Dimitrov, B., & Inaski, I. (2004). *Tribology of abrasive machining processes*. Elsevier. https://doi.org/10.1016/C2010-0-67070-2